TECTONIC AND CLIMATIC INFLUENCES ON BEDROCK CHANNELS TRAVERSING THE CENTRAL ANDES, BOLIVIA

Jonathon F. Syrek

A thesis submitted to the faculty of the University of North Carolina at Chapel Hill in partial fulfillment of the requirements for the degree of Master of Science in the Department of Geological Sciences.

Chapel Hill
2012

Approved by:

Dr. Jason B. Barnes

Dr. Tamlin M. Pavelsky

Dr. Kevin G. Stewart

ABSTRACT

JONATHON F. SYREK: Tectonic and Climatic Influences on Bedrock Channels Traversing the Central Andes, Bolivia
(Under the direction of Jason B. Barnes)

I combine rock strength variations estimated from field data and topographic analyses of 252 channels across the semiarid southern Bolivian Andes to investigate the role of tectonics on knickpoint formation and bedrock channel steepness patterns. Sixty percent (17 of 29) of knickpoints along 4 trunk rivers are spatially correlated with a rock unit transition. Seventy-seven percent (10 of 13) of identifiable knickpoint morphologies (vertical-step versus slope-break) that correlate with a rock unit change match a recently published theoretical framework. Knickpoints in southern Bolivia are only small-scale, local features. Larger, regional steepness patterns are not simply correlated to rock strength, but instead I argue they are primarily influenced by the fold-thrust belt architecture and associated active rock uplift patterns dictated by large-scale basement deformation. In contrast, rivers in northern Bolivia possess more systematic downstream decreases in channel steepness and high profile concavities that reflect strong influences from enhanced orographic precipitation.

ACKNOWLEDGEMENTS

Financial support was provided by a United States Geological Society of America Graduate Student Research Grant and the University Of North Carolina Department Of Geological Sciences' Martin Fund. Further financial support was provided to Jason B. Barnes by a UNC Junior Faculty Development Award.

Many people contributed to the success of this project. First and foremost, I would like to thank my advisor, Dr. Jason Barnes, for his mentorship, knowledge, and patience during the last two years. I could not have asked for better training, and won't ever forget his countless ideas that made the completion of this thesis possible. I thank Dr. Tamlin Pavelsky and Dr. Kevin Stewart for their additional critiques and insights that greatly improved the thesis. I also thank my Bolivian collaborators, Jaime Tito and Sohrab Tawackoli for logistical support while in the field. My colleagues provided invaluable discussions on project ideas and my understanding of geomorphologic and hydrologic concepts. I especially thank George Allen, Maggie Ellis, Colleen Long, Zach Miller, and Caitlin Rushlow. Finally, I thank my parents and sisters for their guidance and unwavering support throughout my graduate studies.

TABLE OF CONTENTS

LIST OF TABLES

Table

LIST OF FIGURES

Figure

CHAPTER 1

INTRODUCTION

Active mountain landscapes are constantly evolving features. In these settings, tectonics, climate, and erosion combine to shape orogen topography that can result in a dynamic coupling between these processes (Stolar et al., 2006; Whipple, 2009; Willett, 1999). Perhaps as a result, the alpine topography itself is thought to reflect the spatiotemporal patterns of differential rock uplift and climate (Wobus et al., 2006a and references therein). It is river incision into rock that dictates the manner and rate at which mountain topography changes (e.g., Kirby and Whipple, in review; Seidl and Dietrich, 1992; Tinkler and Wohl, 1998; Whipple et al., in review). This is because river channels set the relief patterns, are the most efficient mechanisms for transmitting signals of tectonic and climatic change throughout the landscape, and set the boundary conditions for hillslope processes (Whipple and Tucker, 1999). In unglaciated regions devoid of variations in geologic structure, faulting, rock strength, precipitation, rock uplift rate, and sediment flux, bedrock rivers retain smooth, concave up longitudinal profiles (Whipple and Tucker, 1999). However, all mountains contain some of these variations, causing channels to deviate from this idealized form and develop local convexities called knickpoints (e.g., VanLaningham et al., 2006; Walsh et al., 2012; Whipple and Tucker, 1999) or irregular changes in gradient downstream (e.g., Duvall et al., 2004; Whittaker,

2012). Emerging theory suggests that the specific form of a knickpoint can be used to identify the driving force behind it (Haviv et al., 2010; Whipple et al., in review).

Patterns of bedrock river gradients can be a useful tool for ‘reading’ the patterns and rates of rock uplift (e.g., Wobus et al., 2006a). However, the channel gradient response to spatiotemporal changes in rock strength and climate must first be removed to isolate this tectonic uplift rate signal. The central Andes are characterized by significant variations in rock strength, fold-thrust belt structure, and orographic climate patterns (Allmendinger et al., 1997; Horton, 1999; Isacks, 1988; Masek et al., 1994; Montgomery et al., 2001; Norton and Schlunegger, 2011; Schlunegger et al., 2011). In particular, the semiarid climate south of the Bolivian orocline is well suited to investigate the principal effects of across-strike variations in fold-thrust belt architecture (patterns of rock deformation, age, and type) on bedrock river form. Furthermore, minor changes in the mechanical strength of the rocks (McQuarrie and Davis, 2002) suggest limited variation in erodibility within the rock units exposed along strike of the orogen.

The purpose of this paper is to determine the primary controls on local-to-regional scale channel steepness patterns along the eastern flank of the semiarid southern Bolivian Andes. I hypothesize that, since rainfall is reduced, substrate changes cause knickpoints on a local scale (10 m-1 km) and that the thrust belt kinematics, via long-lived rock uplift patterns, affect the regional steepness patterns on the 10 km or larger scale. To test this hypothesis, I (1) quantify bedrock strength with field measurements as proxies for erodibility, (2) determine the location, size, and specific morphology of the major knickpoints along the main stem rivers, (3) analyze long profiles of 252 rivers to map the regional channel steepness patterns, and (4) relate these observations to the fold-thrust

belt structure. Where knickpoint form and cause (via spatial correlation) are identifiable, I use this data to evaluate a recent theoretical framework that predicts the cause of knickpoint formation from its morphology. Finally, I compare my results to channel steepness patterns in subtropical, northern Bolivia to assess effects of orographically enhanced rainfall versus tectonics on channel form.

CHAPTER 2

BEDROCK RIVER MORPHOLOGY

Rivers typically follow a power-law scaling between local channel slope (S) and contributing drainage area (A) (Fig. 1A inset; Flint, 1974; Hack, 1957; Howard and Kerby, 1983; Whipple and Tucker, 1999):

$S=k_sA^{-\theta}$, (1)

where k_s is the channel steepness index and θ the concavity index. The channel steepness index is local channel slope normalized to downstream increases in drainage area. This normalization allows for direct comparison of gradients between river reaches with different drainage areas. However, variations in θ can influence the value of k_s found from a linear regression of log S vs. log A data (Sklar and Dietrich, 1998). To eliminate this autocorrelation, a reference concavity (θ_{ref}) is used to produce a normalized channel steepness index (k_{sn}) (Wobus et al., 2006a). This effectively corrects slope for its dependence on drainage area (Whipple et al., in review). In a steady state landscape, k_{sn} is expected to vary with rock strength, rock uplift rate, and climate. For example, there is an observed positive correlation between k_{sn} and rock uplift rate (Kirby and Whipple, 2001; Kirby et al., 2003; Lague and Davy, 2003; Ouimet et al., 2009; Wobus et al., 2006b), and a negative correlation between k_{sn} and mean annual precipitation (Norton and Schlunegger, 2011). Moreover, some evidence suggests a positive correlation between rock strength and k_{sn} (e.g., Duvall et al., 2004), yet many studies show no measureable

influence of rock strength on k_{sn} (Johnson et al., 2009; Kirby and Ouimet, 2011; Safran et al., 2005; Schlunegger et al., 2011; van der Beek and Bishop, 2003).

A knickpoint is a deviation from the typical power law slope-area scaling in rivers, defined as a distinct inflection point on a long profile followed by a locally high-gradient reach between lower gradients both upstream and downstream of the knickpoint (Burbank and Anderson, 2011; Schoenbohm et al., 2004; Walsh et al., 2012; Whipple and Tucker, 1999). The formation of knickpoints and their upstream migration has been attributed to changes in lithology (Duvall et al., 2004; Snyder et al., 2003), rock uplift rate (Cyr et al., 2010; Karlstrom et al., 2012; Kirby et al., 2003; Snyder et al., 2000), precipitation (Norton and Schlunegger, 2011; Roe et al., 2002), or increased sediment input to the channel (Walsh et al., 2012). Knickpoints commonly take two distinct forms dependent upon the nature of the cause and the river incision mechanics (Whipple et al., in review). These two different knickpoint types, slope break and vertical step, can be identified in plots of local channel slope versus drainage area (Figs. 1B and 1C; Haviv et al., 2010; Whipple et al., in review). Vertical-step knickpoints are local, discrete increases in channel gradient that are recognized as spikes in S-A plots (Fig. 1B; e.g., Goldrick and Bishop, 2007). Stationary vertical-step knickpoints are caused by a change in substrate strength (Whipple et al., in review). Channels locally steepen to erode at the same rate as above the knickpoint. Other vertical-step knickpoints migrate upstream, forming from a discrete baselevel fall caused by stream capture, sea level fall, or a rock uplift pulse (Whipple et al., in review). The upstream propagating incision wave lowers the profile to a new baselevel without a change in k_{sn}. In contrast, a slope-break knickpoint is defined as a permanent, extensive change in channel gradient that separates reaches with different

k_{sn} and is recognized on S-A plots as a permanent upward step (Fig. 1C; e.g., Wobus et al., 2006a). A slope-break knickpoint forms where a river crosses an active fault or a transition in rock uplift rate. The knickpoint remains anchored in place while the contrasting uplift rates remain constant. In addition, slope-break knickpoints form at a contact between different lithologies when the more resistant lithology is spatially extensive. Incision into extensive, stronger rocks downstream typically requires higher equilibrium slopes. Slope-break knickpoints become mobile when tectonic activity on a structure ceases or abruptly increases (see Whipple et al., in review; Wobus et al., 2006a).

Spatiotemporal variations in climate can also affect river long profiles (Fig. 1D; e.g., DiBiase and Whipple, 2011; Roe et al., 2002; Wobus et al., 2010). For graded streams, large concavity values ($\theta>1$) occur where precipitation rates increase downstream (Roe et al., 2002; Schlunegger et al., 2011). Channels respond to orographic precipitation by forming a zone of increased θ, in some cases initiating a tectonic response to increased incision (Fig. 1D). This potential feedback causes the headwater reaches to form high k_{sn} during headwater retreat (Schlunegger et al., 2011).

CHAPTER 3

THE BOLIVIAN ANDES

The Andes span the entire western margin of South America and exhibit a sharp bend near their widest point at ~18°S (Fig. 2; Isacks, 1988). South of the bend, the eastern Andean flank is a fold-thrust belt that descends from ~5000 m to <300 m over ~400 km distance. In Bolivia, the fold-thrust belt is shortened ~326 km and divided into 3 distinct tectonomorphic zones defined by downward steps in mean elevation and upward steps in structural level of exposure (Figs. 2 and 3; Kley et al., 1996; McQuarrie, 2002): The Eastern Cordillera (EC) is comprised of Paleozoic quartzite, weakly metamorphosed sandstone, and shale with minor Tertiary volcanics. EC cover rocks are shortened ~122 km and spacing between thrust sheets averages ~9 km. The Interandean zone (IA) is primarily tightly folded Devonian and Carboniferous sandstone with minor shale and siltstone. Total shortening in the IA is ~96 km with average spacing between thrust sheets ~6 km. The Subandes (SA) contain mostly Carboniferous, Triassic, and Cretaceous sandstone uplifted along narrow (~1-5 km) thrust sheets, separated by Tertiary synorogenic sediments in broad, large wavelength (10-20 km) piggyback basins.

Basement deformation is significant within the Bolivian fold-thrust belt and compliments the exposed deformation in the cover rocks (e.g., Dunn et al., 1995; Elger et al., 2005; Kley, 1999). The large-scale structural and morphological variations across the thrust belt (EC-IA-SA) have been explained by the stacking of two major basement

structures (Fig. 3; Kley, 1996; McQuarrie, 2002; McQuarrie et al., 2005; Müller et al., 2002). Elevated basement in the EC inferred from magnetotelluric data results from the eastward propagation of an upper basement thrust that fed deformation into the cover rocks (Kley, 1999; Kley et al., 1996; McQuarrie and DeCelles, 2001; Schmitz and Kley, 1997). More recently, movement on a lower basement structure initiated passive uplift of the EC and IA and currently feeds deformation to the SA thrust sheets (Kley et al., 1996). Deformation and exhumation began ~40 Ma in the EC, ~20 Ma in the IA, and ~15-10 Ma in the SA (e.g., Barnes and Ehlers, 2009; Ege et al., 2007; McQuarrie, 2002; McQuarrie et al., 2005). Thus, the uplifted thrust-sheet hanging walls in the SA are the only surface structures that are active in the thrust belt over the last ~10 Myrs.

In southern Bolivia, the Grande, Parapeti, and Pilcomayo Basins and their channel networks transport water and sediment eastward across the fold-thrust belt to the foreland (Fig. 2; Barnes and Pelletier, 2006). The channels are bedrock or mixed bedrock-alluvium with variable gradients and discharge. They also traverse orographic precipitation gradients across the central Andes that vary significantly with latitude (Fig. 2 inset; Garreaud and Wallace, 1997). In southern Bolivia, mean rainfall peaks at ~2 m/yr in the IA and decreases to <1 m/yr in the SA and to ≤0.1 m/yr in the EC (Fig. 2 inset; Bookhagen and Strecker, 2008). This moderate climate may help explain partial preservation of an extensive, subhorizontal, low-relief surface (the San Juan del Oro) at ~3800-2000 m elevations in the EC-IA that truncates deformed Paleozoic to Cenozoic bedrock (Gubbels et al., 1993; Kennan et al., 1995; 1997). In contrast, an enhanced latitudinal and orographic precipitation gradient produces mean rainfall peaks up to ~5 m/yr north of the orocline in the Upper Beni Basin. Here, perhaps as a result, a few

channel systems (e.g., Río La Paz) have cut headward through the EC and into the plateau, pushing the drainage divide to the west.

CHAPTER 4

METHODS

Rock Strength

Several factors can influence the resistance of substrate to erosion, an important element in river incision, including rock hardness (strength) and fracture spacing (Duvall et al., 2004; Hack, 1957; Sklar and Dietrich, 2001; Stock and Montgomery, 1999; Whipple et al., 2000a; Whipple et al., 2000b). I quantified both metrics in the field as a proxy for rock erodibility (after Dühnforth et al., 2010; Goudie, 2006; Katz et al., 2000). Schmidt hammer rebound (R) values are comparable to the unconfined compressive strength estimated from laboratory experiments (Selby, 1980). I collected 2829 Schmidt hammer measurements (~40 per site) at 71 sites from all major rock units exposed in the southern basins (Fig. 2). Measurements that yielded a hollow sound, fractured the rock, or recorded an R value <11 were eliminated (after Duvall et al., 2004; Kirby et al., 2003). I did not correct for hammer inclination because these deviations are negligible in comparison to the variability associated with the measurements themselves (Snyder et al., 2003b). Within each major geologic unit (e.g., Ordovician, Silurian), I divided site measurements equally among the different exposed lithologies to define a representative hardness value. I report a mean R value (± 1σ) averaged over n sites from each rock unit (after Katz et al., 2000) (Table 1; details in Appendix).

The degree of fracturing also influences substrate strength (Clarke and Burbank, 2011; Dühnforth et al., 2010; Duvall et al., 2004; Whipple, 2004) because fractures enhance rock surface area exposed to weathering and dissolution, weakening rock (Selby, 1980). I measured fracture spacing using scan lines (after Brooks et al., 1996; Dühnforth et al., 2010; Gillespie et al., 1993) and defined any crack, fault, or bedding plane that crossed the line at a near-perpendicular angle as a fracture. I measured fractures along 4 scan lines of ~1 m each at every site. In most cases, half of the scan lines were measured perpendicular to bedding and half parallel to bedding.

Channel Morphology

I extracted channel slope and drainage area from the hydrologically-conditioned ~90 m Shuttle Radar Topography Mission (USGS HydroSHEDS SRTM) digital elevation model (DEM) dataset (Lehner et al., 2008) with an ArcGIS stream profiler plugin and suite of Matlab scripts (see Kirby et al., 2003; Snyder et al., 2000; Wobus et al., 2006a). I then applied standard sampling and filtering techniques to the DEM and used a $\theta_{ref} = 0.45$ for comparison with previous studies (e.g., Safran et al., 2005; details in Appendix).

Bedrock rivers are channels that incise rock over geologic timescales, even if temporarily covered in alluvium (Whipple et al., in review), which is the case for many channels in southern Bolivia. I focused on the regional, first-order patterns of bedrock river morphology across the region and hence limited my analysis to channels with drainage areas >150 km^2 (252 rivers in southern Bolivia). I then identified the large (>Δ200 m$^{0.9}$ in k_{sn}) knickpoints unassociated with tributary junctions along the 4 main

stem southern rivers (Fig. 2: Ríos Grande, Pilcomayo, Pilaya, and Parapeti) and compared them to a 1:1,000,000-scale geologic map (Armijo et al., 1996) to determine if they are associated with any type of substrate change and/or fault. Where possible, they were also classified as vertical-step or slope-break knickpoints dependent upon their form in S-A plots (after Figs. 1B and 1C). Finally, I compared regional steepness (k_{sn}) patterns to the tectonic architecture, kinematics, and climate of the thrust belt.

CHAPTER 5

RESULTS

Rock Strength

Schmidt hammer measurements show rock hardness does not correlate with age, yet there are significant differences within and between the major mapped rock units (Fig. 4, Table 1). The data suggest 2 distinct groups (vertical lines in Fig. 4): a 'hard' group that includes the Devonian, Cretaceous, and Ordovician quartzite and sandstone units (mean R = 52 ± 6), and a 'soft' group that includes the other Ordovician subset (shale/slate/siltstone), Silurian, Carboniferous, Triassic, and Tertiary units (mean R = 36 ± 4). In detail, the Devonian rocks are the strongest (R = 55 ± 7) and Ordovician shale, slate, and siltstones are the weakest (R = 27 ± 10).

Fracture measurements show that (a) spacing inversely correlates with rock unit age and (b) there are 3 statistically different classes: low, moderate, and high mean fracture spacing (vertical lines in Fig. 4, Table 1). I included bedding planes in the fracture spacing measurements such that the fracture spacing reflects the combined result of average bed thickness and degree of strain for each rock unit. The Ordovician, Silurian, and Devonian units have low spacing (mean 3 ± 1 cm), the Carboniferous, Cretaceous, and Tertiary sedimentary units moderate spacing (14 ± 2 cm), and the Triassic and Tertiary volcanic units high spacing (60 ± 10 cm). I assigned a minimum spacing of 100 cm to 2 Triassic sites of massive sandstones devoid of fractures. I

expected a positive correlation between fracture spacing and rock hardness (after Stimpson, 1980), but my results do not show this (Fig. 5).

The combined fracture spacing and Schmidt hammer data suggest the rock units can be put into 2 rock strength groups, a proxy for rock erodibility (after Selby, 1980). The weaker rocks are the Ordovician shale, slate, and siltstone and the Silurian, Carboniferous, and Tertiary sediments. The stronger rocks are the Ordovician quartzite, Devonian, Triassic, and Cretaceous sediments, and Tertiary volcanics. These collective results suggest no systematic variation in strength across strike or with rock age.

Knickpoints

Many (29) large knickpoints exist along the 4 principal rivers traversing the southern basins. Sixty-two percent (18 of 29) of them correlate with a rock unit contact and 52% (15 of 29) correlate with a mapped fault. Only 17% (5 of 29) of the knickpoints correlate with a fault and no rock unit contact. Along the Río Yurimata (Río Pilcomayo tributary), a knickpoint correlates with a thin (~4 km), fault-bounded section of strong Cretaceous sandstone between weak Ordovician slate upstream and downstream (Fig. 6). The Cretaceous sandstone correlates with a river profile convexity and a steepened reach (dashed line in Fig. 6B). Here, large (1-5 m) sandstone boulders are the primary bedload size of the steepened reach within the Cretaceous and then reduce to cobbles and smaller within the Silurian sediments (Fig. 6A). The Río Grande has 9 knickpoints and 5 of them correspond to rock unit contacts (Fig. 6A). Three of the 5 knickpoints are in the IA, including the maximum k_{sn}, aligned with a transition between Silurian rock and Ordovician quartzite. Five of 9 knickpoints also correlate with a fault, including 2 not at a

rock unit contact. The largest knickpoint reaches a k_{sn} near 600 $m^{0.9}$ (1 in Fig. 7A). The Río Parapeti flows almost entirely within the SA, crossing multiple uplifted thrust sheets. There are 4 knickpoints, 3 correlate with rock unit contacts and 3 with mapped faults. Two of 4 are knickpoints that correspond with uplifted thrust sheets. The Río Pilcomayo has 11 knickpoints, 8 of which correspond to rock unit contacts (Fig. 7B) and 4 of the 11 with a fault. Only 1 knickpoint at a fault is not near a rock unit contact. Most (7) of the knickpoints are in the EC, of which 4 occur at a contact with Ordovician rock. Maximum k_{sn} on the Río Pilcomayo is >800 $m^{0.9}$ at an Ordovician-Silurian contact in the IA, and remains high throughout the Silurian unit (2 in Fig. 7B). Farther south, the Río Pilaya has 5 knickpoints upstream of its confluence with the Río Pilcomayo. Two knickpoints correspond to rock unit contacts and 3 with faults. The 2 knickpoints correlated with rock unit contacts are in the EC and both are at thrust faults. One corresponds with the edge of the Los Frailes ignimbrites and the other with a thin, isolated Cretaceous unit (km 40 & 140; Fig. 7C).

About half (13 of 25) of the knickpoints are distinct enough to be classified as slope break or vertical step in form. Three knickpoints on the Río Grande are distinct (arrows in Fig. 7A). The first 2 are slope-break knickpoints at a rock unit contact (km 90 and 360; Fig. 7A) where the downstream unit is spatially extensive and both are also at thrust faults. The third is a vertical-step knickpoint at a rock unit contact where the weaker Ordovician section is extensive (~5 km). There are 7 distinct knickpoints on the Río Pilcomayo (arrows in Fig. 7B): 3 are vertical step, 2 of which correspond to rock unit contacts and 1 of those also at a fault. The other is at neither a rock unit contact nor a surface fault. The other 4 are slope-break knickpoints that all coincide with rock unit

contacts and 2 of which are also at faults. On the Río Pilaya, 3 knickpoint forms are identifiable (arrows in Fig. 7C). The first is a slope break that is located on a rock unit contact between the Los Frailes ignimbrites and an extensive Silurian section downstream. Another is a vertical-step knickpoint (at km 140 in Fig. 7C) at a fault-bounded, thin Cretaceous section between locally stronger Ordovician rocks. The third is a slope-break knickpoint upstream of a section of high k_{sn} (>3500 $m^{0.9}$) within the Ordovician. Other knickpoints are identifiable in S-A plots, but the data is too coarse to accurately assess their form. Knickpoints occur regardless of whether weak or strong rock is downstream of the knickpoint because any change in substrate requires a change in equilibrium grade. I conclude that 5 of 6 slope-break knickpoints and 3 vertical-step knickpoints are related to a lithologic contact. It is also possible that 4 slope-break knickpoints and 2 vertical-step knickpoints are related to mapped faults.

The largest knickpoint (~35 km in length) is on the Río Pilaya and is not related to a major rock unit change (3 in Fig. 7C). Here the river traverses interbedded Ordovician slate and quartzite. The lower end of the knickpoint occurs ~50 km downstream of the San Juan del Oro tributary junction and ~15 km west of the EC-IA boundary (3 in Fig. 8). Channel elevation drops ~1 km with maximum k_{sn} ~3500 $m^{0.9}$ and mean k_{sn} ~720 $m^{0.9}$ throughout the knickpoint.

Regional Steepness Patterns

A k_{sn} map reveals large-scale (10^{1-2} km) patterns of channel steepness for 252 rivers across southern Bolivia (Fig. 8, Table 1). I identify 3 main zones of channel steepness: (1) a zone of low k_{sn} throughout most of the EC, transitioning to (2) a N-S

zone (~90 wide) of high k_{sn} that roughly follows the easternmost EC and entire IA and widens to ~200 km in the northern Grande Basin, and (3) a low-k_{sn} zone south of the Río Grande in the SA. Most rivers in the SA flow within piggyback basins and reveal few perturbations to a graded profile. Locally steepened reaches correspond to rivers flowing across strike over uplifted thrust-sheet hanging walls that also expose mostly pre-Tertiary rocks.

I compared mean k_{sn} and estimated the strength for each rock unit to evaluate the effect of rock erodibility on regional k_{sn} patterns (Table 1). I expected rock strength to be positively correlated with k_{sn} (e.g., Duvall et al., 2004) because the majority of steep reaches occur within strong Devonian rock. For strong rock, the stream must steepen to increase its stream power, and hence its ability to incise (e.g., Whipple, 2004). However, my results show mean steepness indices are the same within error for every major mapped rock unit (Fig. 9), revealing rock strength is not a factor at regional ($10^{1\text{-}2}$ km) scales in southern Bolivia, similar to other studies (e.g., Kirby and Ouimet, 2011; Schlunegger et al., 2011).

CHAPTER 6

DISCUSSION

Knickpoint Form and Cause

Most knickpoints can be explained by a lithologic change (~62%) and/or a fault (~52%). This suggests that the tectonic architecture of the thrust belt imparts the largest influence on channel morphologies draining the eastern Andean flank in southern Bolivia. However, 7 additional knickpoints do not correlate with either feature, but this does not eliminate the possibility they result from faulting or a lithologic change. For example, these knickpoints may result from strength variations within a single rock unit at a scale smaller than the mapped geology. Second, these knickpoints could be migratory, in which case the cause (e.g. baselevel change) may be located downstream. Given the structural complexity of the thrust belt and the transient nature of channel steepness variations, I consider the channels to be significantly influenced by the thrust belt architecture because >50% of knickpoints in southern Bolivia can be directly related to tectonic discontinuities. The geomorphic implication is that local-scale, abrupt changes in channel gradients will continue to reflect substrate changes in fold-thrust belts long after the surface deformation has ceased (~10 Ma or more in the EC and IA).

Most (77%) of the large knickpoints I identified corroborate recently proposed theory that links form and cause (Figs. 1 and 7; Haviv et al., 2010). All 6 knickpoints (4 slope break, 2 vertical step) on the Ríos Grande and Pilaya, where knickpoint form is

identifiable, match the theory. Along the Río Pilcomayo, on the other hand, 3 of 7 knickpoints do not agree with the theory. Although it is unclear why, I note uncertainties may result from inaccuracies on the geologic map or misinterpretation of knickpoints due to DEM artifacts. Slope-break knickpoints are thought to form where the stronger unit is extensive and vertical-step knickpoints are thought to form along small, local patches of stronger units (Whipple et al., in review). The slope-break knickpoints I observe coincide with where the stronger units are ≥5 km wide; however, there is no definition quantifying the length scale for a rock unit to be considered extensive. I expect this boundary to fluctuate dependent upon the contrast in rock strength at the contact and external forces (e.g., climate, tectonics, and sediment flux). Regardless, this study provides validation for the relationship between knickpoint morphology and cause (Haviv et al., 2010; Whipple et al., in review).

Regional Steepness (k_{sn}) and Rock Uplift Patterns

Mean k_{sn} patterns show no correlation with rock strength at large ($10^{1\text{-}2}$ km) length scales in southern Bolivia (Fig. 9), suggesting minimal influence on regional-scale k_{sn} patterns. The narrow, high-k_{sn} zone is primarily within the IA and parallels the fold-thrust belt structure along strike (Fig. 8). Two reaches with the highest k_{sn} are both ~20 km west of the EC-IA boundary (2 and 3 in Fig. 8). The relatively high-relief IA receives locally high precipitation (up to ~2 m/yr; Fig. 2 inset) and thus I might expect to see increased concavity as well (Roe et al., 2002; Zaprowski et al., 2005). However, rivers crossing the high-k_{sn} zone possess below average concavities relative to rivers in northern Bolivia.

These observations thus suggest some other type of tectonic influence besides substrate change, such as differential rock uplift rate.

On the SW corner of the high-k_{sn} zone is a 40 km reach of the Río Pilaya that drops ~1 km and displays the highest k_{sn} values near 3500 $m^{0.9}$ (3 in Figs. 7C and 8). It is unlikely that rock strength variations cause this knickpoint because lithologic effects are unlikely to create 1 km of relief (Whittaker et al., 2008) and it traverses both weak and strong Ordovician rocks. Existing balanced sections place ramps on basement faults as well as a duplex directly below this knickpoint (dashed box in Fig. 3; Kley et al., 1996; McQuarrie, 2002). Since ~40 Ma, there has been movement on various basement structures concentrated at this location. Continuing motion along the lower basement thrust since ≤~20-10 Ma is responsible for uplifting the easternmost EC via a ramp. Passive uplift of the IA results via emplacement of a basement wedge while transferring deformation from the basement into the SA thrust sheets (e.g., McQuarrie, 2002). The kinematics may be maintaining a long-lived west-to-east gradient in relative rock uplift rate at the easternmost EC, hence causing the knickpoint (see also Barke, 2004). Thus, the regional extent of the high-k_{sn} zone and its lack of a correlation with mapped rock units, the low channel concavity, and the spatial correlation with active basement deformation suggest spatial variations in rock uplift rate may be influencing the regional-scale k_{sn} patterns in southern Bolivia.

If the regional steepness patterns are the product of a long-lived uplift gradient, the Río Pilaya knickpoint should be a static feature (Whipple et al., in review). Transient knickpoints propagate more quickly along main stem rivers because of higher discharge relative to small tributaries (Foster and Kelsey, 2012). Thus, knickpoints migrating

through a channel network that are related to the same mechanism (e.g., differential rock uplift rate) occur at similar elevations (Niemann et al., 2001; Wobus et al., 2006a). If the large Río Pilaya knickpoint is transient, I expect to see tributary knickpoints at similar elevations. I analyzed S-A scaling for 6 tributaries downstream of the main knickpoint on the Río Pilaya to assess if it is a migrating or stationary feature.

Half (3 of 6) of the Río Pilaya tributaries that link immediately downstream of the main knickpoint contain knickpoints themselves, but all at different elevations (Fig. 10). One of the knickpoints (river 6 in Fig. 10) is likely related to a rock unit change from Devonian sandstone to Cretaceous quartzite. Knickpoints on 2 tributaries are at ~2500 m and ~2200 m, respectively, whereas the Pilaya knickpoint is at ~2000 m. However, the other 3 tributaries have no knickpoints. Even if the 2 tributary knickpoint elevations roughly correlate with the main Pilaya knickpoint, I would still expect to see them on the other tributaries. I may expect lithologic variations to cause knickpoints to migrate at different rates, but many of the tributaries (rivers 2-5 in Fig. 10) flow only through Devonian rock, therefore it is unlikely that lithologic variations can explain a lack of knickpoints along rivers 2-5. In addition, the Devonian rock is strong (Table 1), so knickpoints should propagate upstream at a slower rate than they would in weaker rock, and thus they would be at lower elevations than the Pilaya knickpoint. Furthermore, these tributaries are close to the Pilaya knickpoint and hence precipitation patterns are similar along all of them. In conclusion, I argue that the main Pilaya knickpoint is stationary in nature and the result of long-lived differential rock uplift, consistent with prior work (Barke, 2004; Barke and Lamb, 2006).

Previous studies along the eastern margin of the Tibetan Plateau adjacent to the Sichuan Basin show similar k_{sn} patterns to southern Bolivia. A sharp, linear physiographic transition in central Nepal at the location of the Main Central Thrust correlates with an abrupt increase in k_{sn} values (Kirby and Ouimet, 2011; Kirby et al., 2003). These patterns are attributed to duplex growth associated with accretion across a deep-seated fault ramp (Wobus et al., 2006c) or a surface breaking thrust fault (Kirby and Whipple, in review). I suggest the situation is similar in southern Bolivia. Therefore, the kinematics of basement deformation may play a key role in influencing steepness patterns of bedrock rivers traversing active orogens.

Comparison to Northern Bolivian Andes

I compare my results to the Upper Beni Basin in northern Bolivia to evaluate the influence of a dramatically enhanced rainfall gradient on k_{sn} and θ patterns. The topographic front along the Upper Beni Basin coincides with a sharp precipitation gradient across the EC (Figs. 2 and 11; Masek et al., 1994) that may have existed since ~15-11 Ma (Barnes et al., in press). Empirical results suggest a correlation between θ and high mean annual rainfall (Schlunegger et al., 2011; Zaprowski et al., 2005) and theoretical studies propose that increased precipitation along the front reduces k_{sn} downstream (e.g., Roe et al., 2002; Whipple et al., 1999). Using a normalized contributing drainage area, downstream increases in discharge are largely the effect of increased precipitation, especially in the EC. Channel morphologies in the Upper Beni Basin show high-k_{sn} profiles at low drainage areas, low k_{sn} at high drainage areas (Fig. 11A), and high concavity, particularly along the reaches directly affected by orographic

precipitation (Fig. 1D, see also Safran et al., 2005; Schlunegger et al., 2011). These characteristics may reflect a landscape that is also responding to tectonic perturbations, but the channel morphology signal of those perturbations is muted by the enhanced orographic precipitation in comparison to southern Bolivia. Instead, the northern rivers have enough discharge, and hence stream power (e.g., Horton, 1999; Whipple and Tucker, 1999), to sustain more uniformly graded profiles despite similar variations in thrust-belt architecture and rock uplift patterns that exist in the south (cf. Barnes et al., 2008; McQuarrie et al., 2008a). This is not to say that knickpoints do not exist along the northern rivers (see Schlunegger et al., 2011), just that they are more modest features relative to those in the south (Fig. 11A). This idea is consistent with the Upper Beni Basin as a climatically driven landscape (Masek et al., 1994; Norton and Schlunegger, 2011; Safran et al., 2005; Schlunegger et al., 2011).

The northern Río Coroico exhibits larger θ than any southern Bolivian trunk river (0.52 ± 0.03; Fig. 11A), suggesting orographic precipitation is altering river profiles in the north (Fig. 1D). Concavity systematically decreases to the south from the Upper Beni Basin, in concert with maximum mean annual precipitation rates (Fig. 11; Bookhagen and Strecker, 2008), despite minimal latitudinal variations in rock strength (e.g., McQuarrie and Davis, 2002; McQuarrie et al., 2008b). From north to south, the Río Grande (θ = 0.32 ± 0.022), Río Pilcomayo (θ = 0.19 ± 0.027), and Río Pilaya (θ = 0.16 ± 0.032) all show low concavity relative to typical mean values from other locations (Fig. 11A; cf., Cyr et al., 2010; Duvall et al., 2004; Kirby and Whipple, 2001; Kirby et al., 2003). Upper Beni Basin channels receive rainfall focused in the EC and reflect a response to surface uplift in upstream reaches (Safran et al., 2005; Schlunegger et al.,

2011). A stream power model demonstrates that enhanced precipitation can increase incision, effectively reducing a river's gradient downstream (e.g., Bookhagen and Strecker, 2012; Roe et al., 2002; Whipple et al., 1999). The Upper Beni Basin results are consistent with this model. Fold-thrust belt kinematics are similar along strike, therefore a regional knickpoint located in the south and a lack of such prominent knickpoints in the Upper Beni Basin suggest climate is an important factor influencing river profiles in the north.

Channel Steepness Patterns in Orogens

My results suggest 2 distinct scales of channel steepness patterns. At a local scale (<~10 km), knickpoints in bedrock rivers traversing fold-thrust belts may result from its structural architecture even in specific areas devoid of near-surface active tectonics. For example, in the active Santa Ynez Mountains in California, rock strength variations affect both concavity and k_{sn} at local length scales (Duvall et al., 2004). Also, strength variations between massive quartzite and more highly fractured rocks in western Scotland have an effect on channel slope at the reach scale, but not as much on a catchment scale (Jansen et al., 2010). These studies demonstrate that my results in southern Bolivia are not unique, but in fact lithologic variations in an array of settings affect river morphology at similarly small, local length scales.

At a regional scale (>~10 km), I observe channel steepness patterns that vary differently depending on whether tectonics or climate exerts the dominant influence. A systematic decrease in k_{sn} patterns downstream is likely a result of enhanced orographic precipitation (Schlunegger et al., 2011). In contrast, nonsystematic changes in k_{sn} patterns

downstream, such as the intermediate zone of high steepness in southern Bolivia, may be the result of tectonic processes. The southern margin of the Tibetan Plateau shows similar features to the tropical, northern Bolivian Andes, including a steep front with high peaks at a plateau edge and comparable precipitation patterns (Masek et al., 1994; Bookhagen and Burbank, 2006; Bookhagen and Strecker, 2008). One hypothesis is that the current topography of the northern Bolivian Andes and Himalayan front result from enhanced orographic precipitation (e.g., Masek et al., 1994). However, k_{sn} patterns along the Himalayan front are inconsistent with those expected from enhanced orographic precipitation in the absence of differential rock uplift (Wobus et al., 2006c). Instead, the river profiles suggest a zone of differential rock uplift (Wobus et al., 2006c) similar to the rivers in southern Bolivia. This underscores the importance that subsurface tectonics may play in affecting the regional-scale form of river long profiles traversing active orogens.

CHAPTER 7

SUMMARY AND CONCLUSIONS

I analyzed bedrock river profiles to quantify channel steepness patterns across the semiarid southern Bolivian Andes. Field measurements show that the region is characterized by distinctive rock strength variations, determined by the fold-thrust belt architecture. Sixty-two percent of large (> $\Delta 200$ $m^{0.9}$) knickpoints along the main stem rivers correlate with changes in major rock units, and hence strength. Fifty-two percent of all knickpoints correlate with a mapped fault, but only 14% are at a fault with no rock unit contact. I also found that 77% of the large knickpoints that I could classify as 1 of 2 end-member morphologies (vertical step, slope break) are consistent with theory that relates form to cause (Haviv et al., 2010). I show for southern Bolivia, 5 of 6 slope-break knickpoints are caused by lithologic changes where the stronger rock is spatially extensive. The other knickpoint is above basement thrust ramps and duplexing on the Río Pilaya. Three vertical-step knickpoints are related to lithologic changes where the stronger unit is small in extent. Regional steepness (k_{sn}) patterns display a steep zone that parallels strike across the entire IA region. This zone becomes steeper in the southern Pilcomayo Basin, reaching k_{sn} near 3500 $m^{0.9}$ at the Río Pilaya knickpoint. I attribute this high-k_{sn} zone to movement along basement structures that have created long-lived, continued differential rock uplift. Finally, rivers in the northern Upper Beni Basin display high-k_{sn} profiles near the headwaters, low k_{sn} at high drainage areas, and high concavities

despite traversing similar thrust-belt architecture, but significantly enhanced orographic rainfall patterns. I suggest that increased precipitation in the north decreases channel steepness downstream and increases the concavity of the profile, tempering the signals of tectonic or lithologic variations so prevalent in the south. I conclude that river profile analyses can be used to distinguish between the primary factors controlling river morphology in the central Andes. These patterns can then be used to help decipher river patterns in other fold-thrust belts such as the Himalayan front.

Table 1. Thrust-belt stratigraphy, strength measurements, and mean k_{sn}

Age	Lithology* (in order of abundance)	Mean R value†	Strength classification§	Fracture spacing (cm)	Mean k_{sn} ($m^{0.9}$)
Ordovician	Quartzite	51 (160)	Strong		
Ordovician	Siltstone Shale Slate	27 (200)	Very Weak	3 ± 3	138.2 ± 171.2
Silurian	Shale Sandstone Diamictite	41 (199)	Moderate	3 ± 2	154.5 ± 129.1
Devonian	Sandstone Shale	55 (200)	Strong	4 ± 6	131.1 ± 77.6
Carboniferous	Sandstone Shale Quartzite Siltstone	36 (160)	Weak	12 ± 9	96.2 ± 64.4
Triassic	Sandstone	36 (80)	Weak	70	90.8 ± 76.8
Cretaceous	Sandstone Siltstone Shale	50 (160)	Strong	14 ± 9	112.8 ± 91.2
Tertiary sediments	Sandstone Conglomerate Shale	38 (140)	Weak	18 ± 17	70.7± 57.8
Tertiary volcanics	Tuff	36 (115)	Weak	50 ± 13	84.2 ± 72.2

*Lithology from Dunn et al. (1995) and McQuarrie (2002)
†Number of measurements in parentheses
§Modified from Selby (1980)

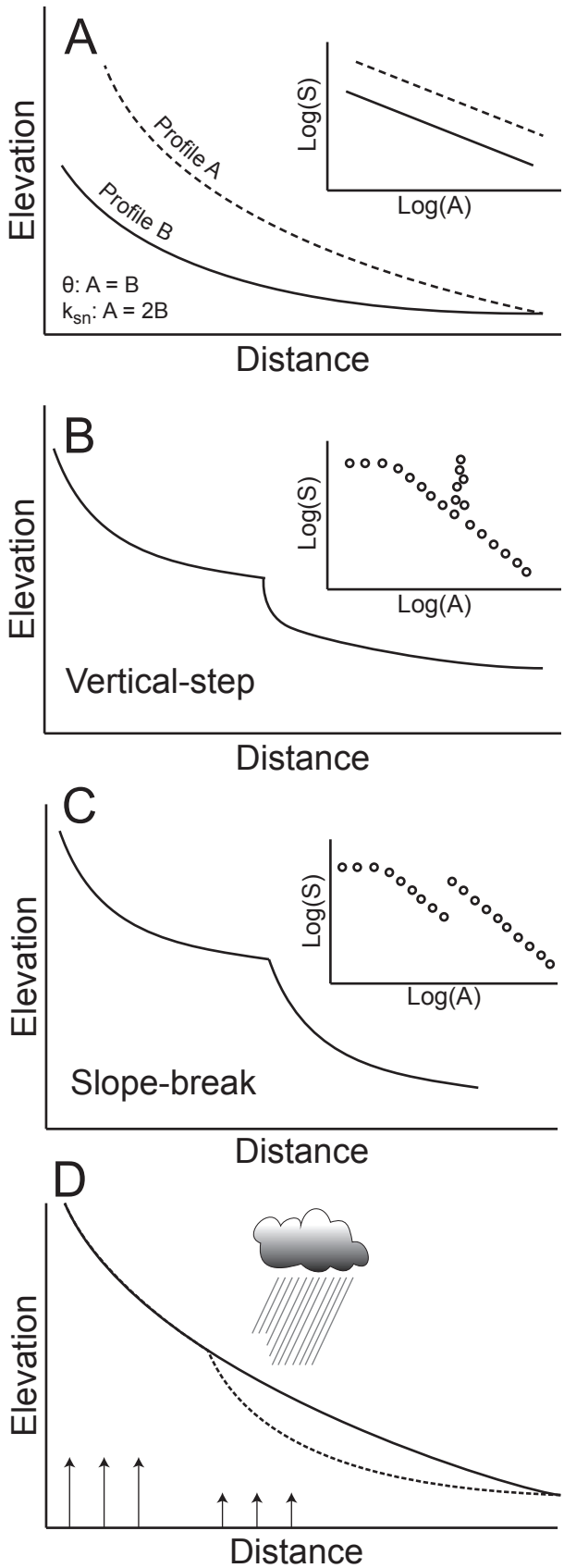

Figure 1. Idealized river long profiles and their response to tectonic and climatic forcing. Long profile and slope-area data (insets) for: (A) two equilibrium profiles with different steepness indices and the same concavity (modified from Duvall et al., 2004), (B) a vertical-step knickpoint and (C) a slope-break knickpoint (modified from Whipple et al., in review). (D) Effect of focused orographic precipitation or differential rock uplift rate on channel long profiles (simplified from Norton & Schlunegger, 2011). Increased rainfall causes channels to increase their concavity. Differential rock uplift rate causes a convex up reach to form. Solid black line is initial profile form, dashed line is profile affected by enhanced precipitation or differential rock uplift rate (arrows).

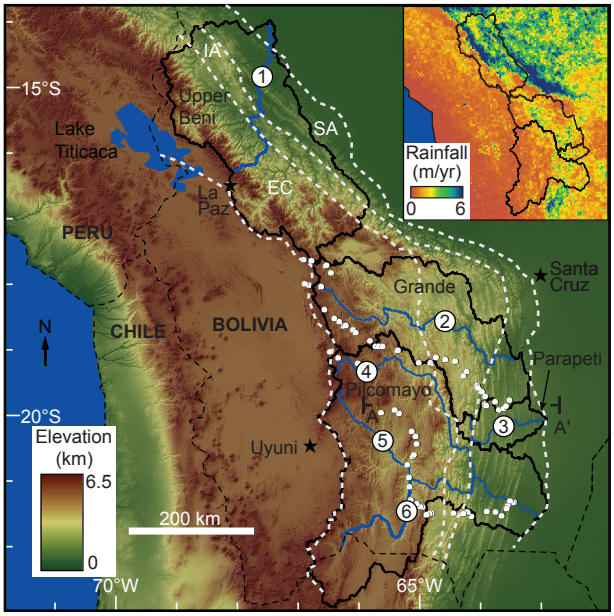

Figure 2. Bolivian Andes topography, thrust belt structure, hydrology, and climate. Major montane basins (solid black lines), trunk rivers (blue lines; after Barnes and Pelletier, 2006), and tectonomorphic zones (dashed white lines; modified from McQuarrie, 2002): EC, Eastern Cordillera; IA, Interandean zone; SA, Subandes. Rivers: 1, Río Coroico; 2, Río Grande; 3, Río Parapeti; 4, Río Pilcomayo; 5: Río Pilaya; 6: Río San Juan del Oro. Small white circles indicate data collection sites. Inset is mean annual rainfall estimated from 1998-2006 TRMM data (Bookhagen and Strecker, 2008).

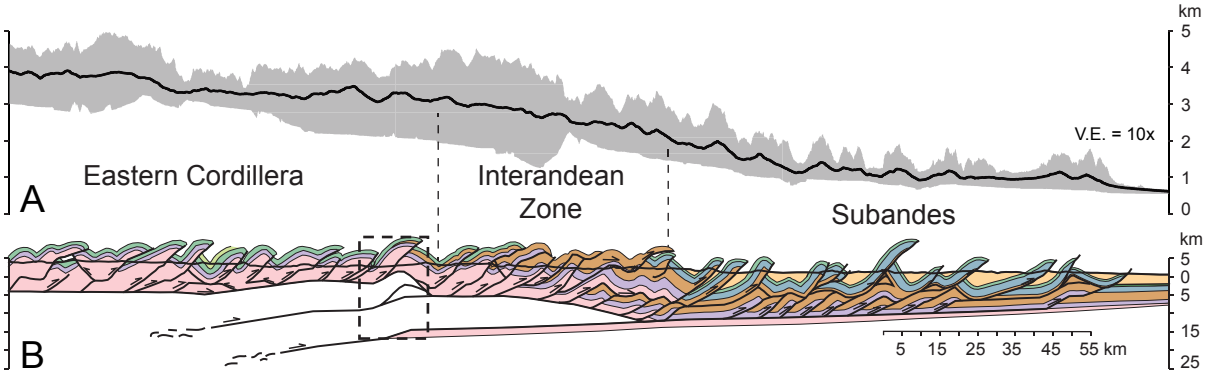

Figure 3. Regional topography and structure of the thrust belt across southern Bolivia (location A-A' in Fig. 2). (A) 100-km-wide swath profile of maximum, mean, and minimum elevations. (B) Geologic cross section showing the linked surface and basement deformation (simplified from McQuarrie, 2002). Geologic map legend is in Figure 8B. Tectonomorphic boundaries are the vertical, dashed lines. Black, dashed box is the location of the regional increased channel steepness above the basement thrust-sheet ramp discussed in the text.

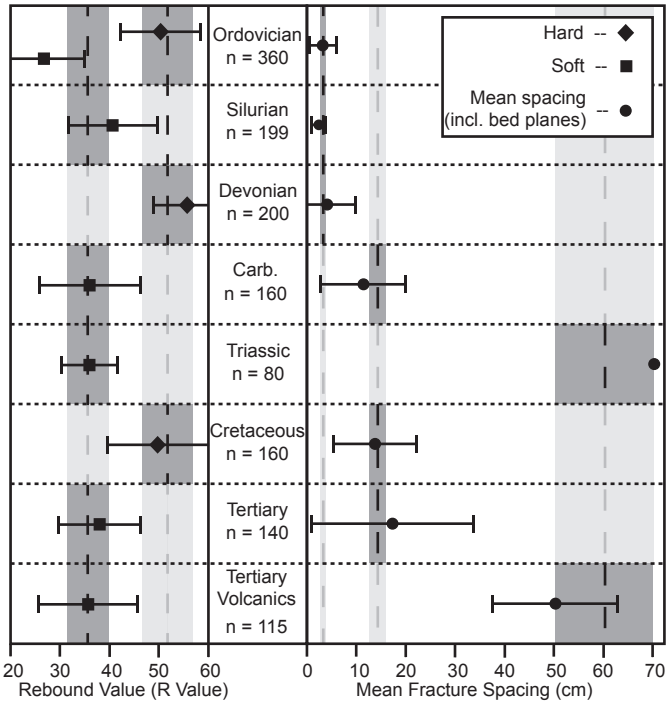

Figure 4. Rock strength proxy measurements for units exposed across southern Bolivia (Table 1). n = number of Schmidt hammer measurements. Mean R values (± 1σ) show a distinct 'hard' and 'soft' group (vertical dashed lines, shaded bar is ± 1 SE). Mean fracture spacing indicates rock units can be divided into three distinct groups. No error bars are shown for the Triassic fracture spacing because the estimate is qualitative.

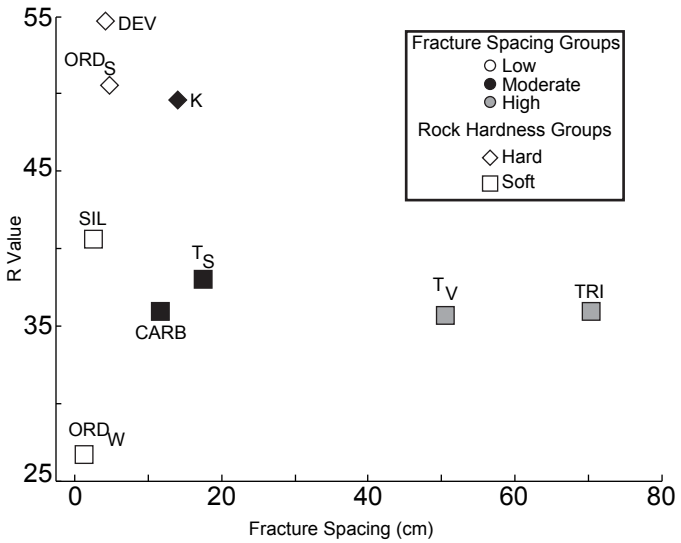

Figure 5. Mean fracture spacing versus mean Schmidt hammer R value for each rock unit. Shape of each marker represents the hardness dependent upon R value (Fig. 4) and marker shading represents the fracture spacing group (Fig. 4). The data show no correlation between fracture spacing and R value.

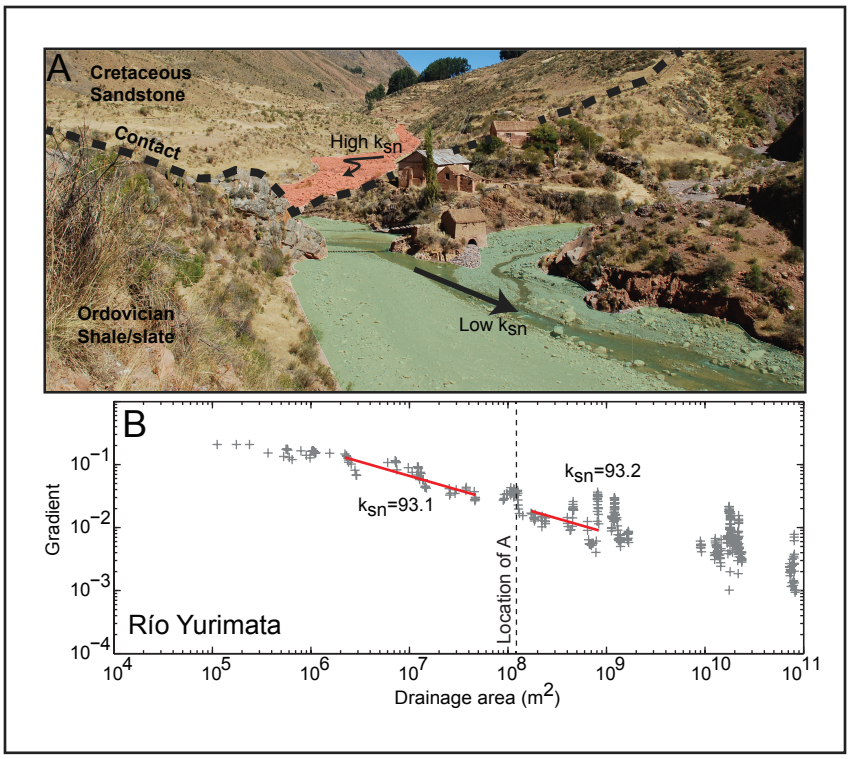

Figure 6. Example of vertical-step knickpoint on the Río Yurimata, a tributary to the Río Pilcomayo (location in Fig. 8B). (A) Photo of channel traversing from strong Cretaceous sandstone to weak Ordovician slaty shale (house for scale). Red indicates the high ksn reach, green the low ksn reaches. Mean bedload grain size is larger in the high ksn reach. (B) Slope-area plot for Río Yurimata. Red lines are best-fit regression (with θref = 0.45) used to calculate ksn. Dashed line is location of vertical-step knickpoint in A.

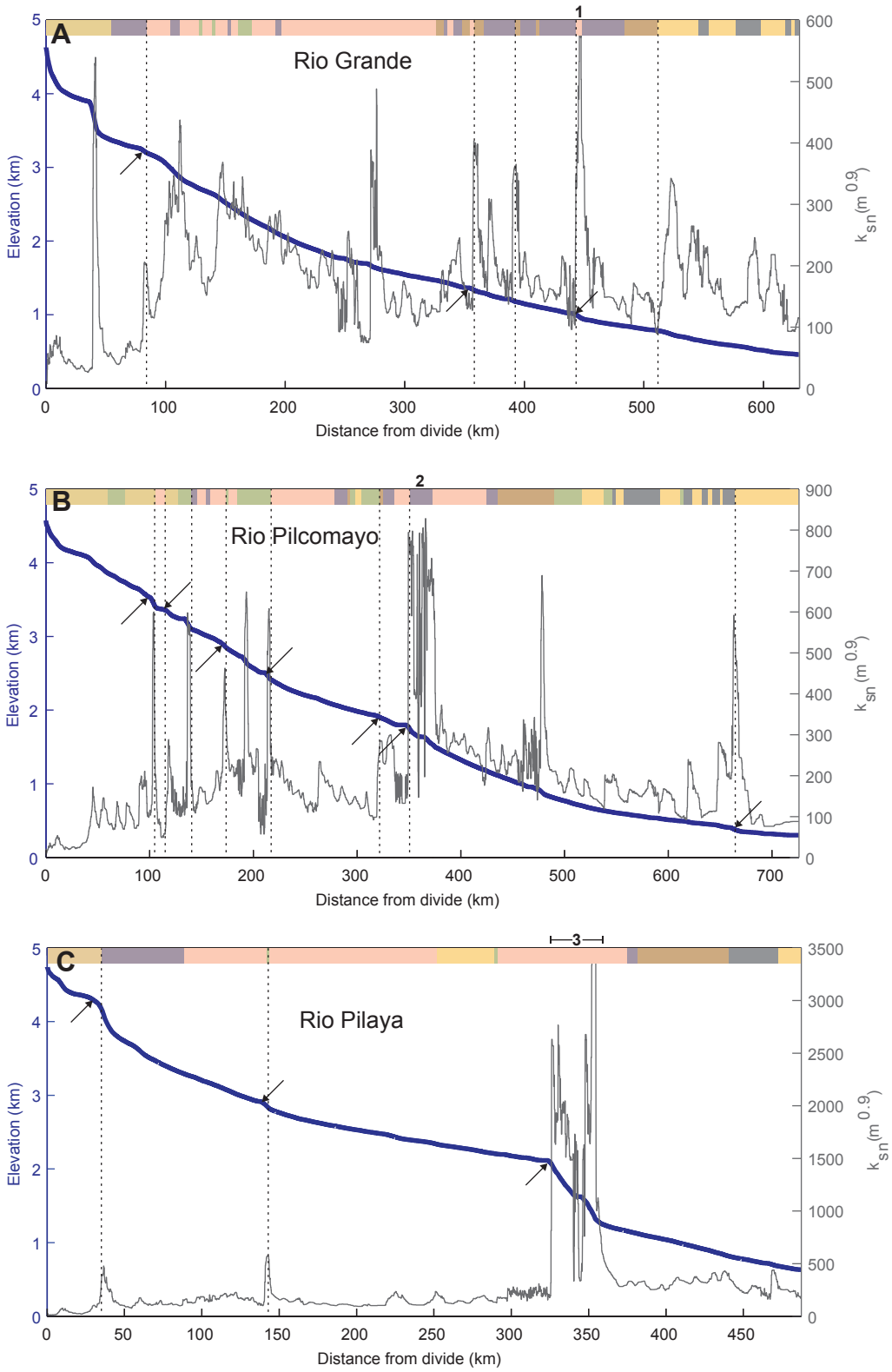
A
Rio Grande
1
Elevation (km)
Distance from divide (km)
k_{sn} ($m^{0.9}$)
B
Rio Pilcomayo
2
Elevation (km)
Distance from divide (km)
k_{sn} ($m^{0.9}$)
C
Rio Pilaya
3
Elevation (km)
Distance from divide (km)
k_{sn} ($m^{0.9}$)

Figure 7. Longitudinal profile (blue line), and ksn (grey line) vs. distance downstream for Ríos (A) Grande, (B) Pilcomayo, and (C) Pilaya. Colors above the profiles are rock units exposed at that location and match the geologic map in Fig. 8B. Dashed vertical lines indicate a transition in rock unit that is spatially aligned with knickpoint on river. Black arrows indicate knickpoints correctly identified as vertical step (arrows above profile) or slope break (arrows below profile). Pink=Ordovician; Purple=Silurian; Dark Brown=Devonian; Grey=Carboniferous and Triassic; Green=Cretaceous; Yellow=Tertiary sediments; Light Brown=Tertiary volcanics.

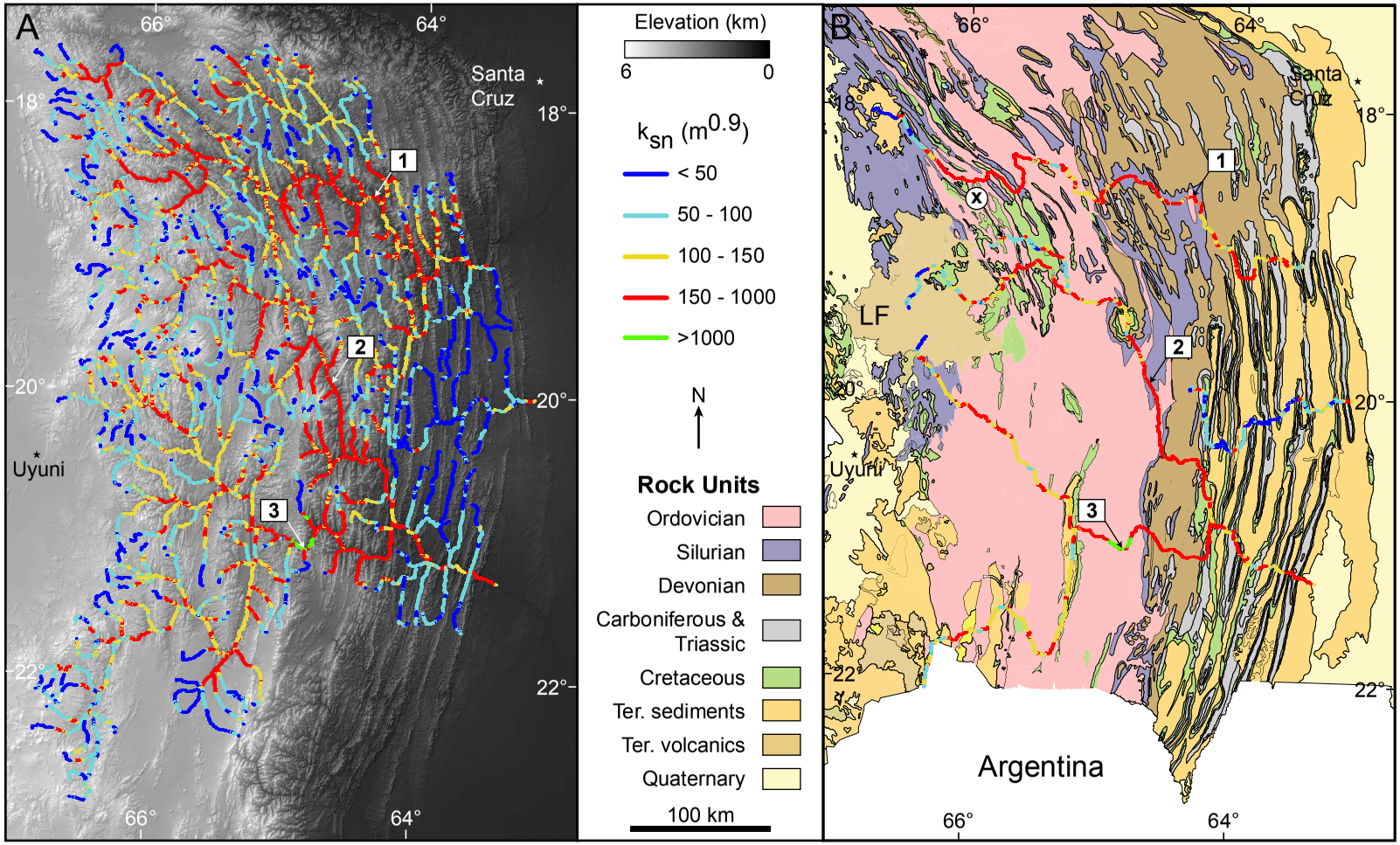

Figure 8. Topography, channel steepness (ksn), and geology across southern Bolivia. (A) Channel steepness and 90 m SRTM topography (Lehner et al., 2008) with prominent knickpoints indicated (1-3). (B) Trunk-stream ksn overlying the thrust-belt geology simplified from a 1:1,000,000 scale map (Armijo et al., 1996). We grouped Carboniferous and Triassic together because they outcrop adjacent to each other and exhibit similar strength. X is location of the knickpoint in Fig. 6. LF, Los Frailes volcanic field; Ter., Tertiary.

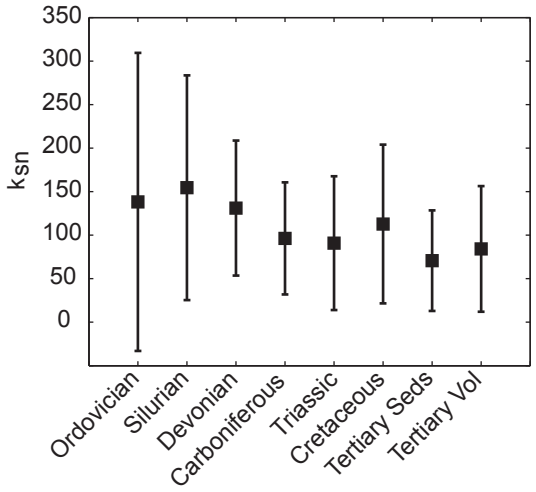

Figure 9. Mean ksn for all southern Bolivian rivers within each rock unit. Vertical bars represent 1σ error. Large errors are present because of a very large range of ksn within each rock unit.

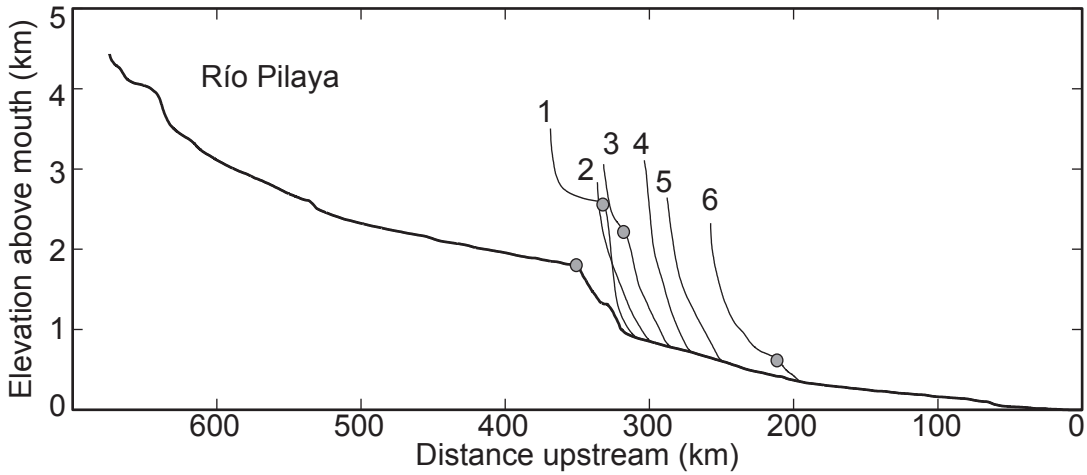

Figure 10. Composite longitudinal profiles and profile reconstruction of the Río Pilaya and its tributaries. Longitudinal profiles of the Río Pilaya and 6 tributaries immediately downstream of the large knickpoint. Circles represent knickpoint locations on the profiles. Numbers represent the tributaries in numerical order from closest to farthest downstream of the main stem knickpoint.

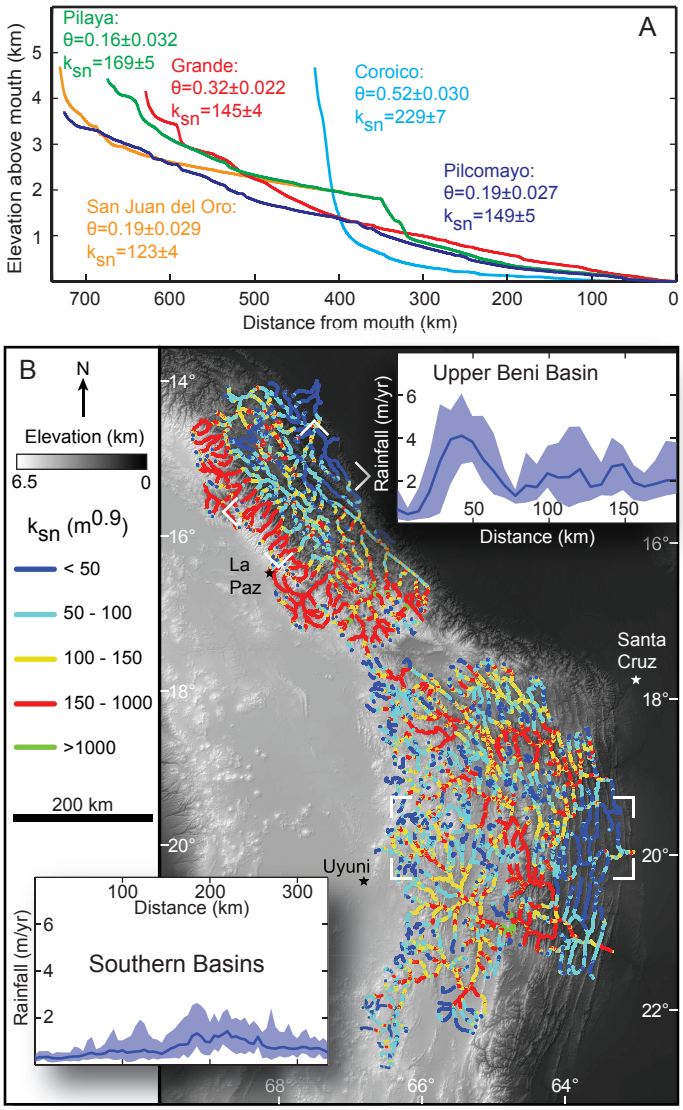

Figure 11. Bolivian Andes main stem long profiles, topography, channel steepness (ksn), and mean annual precipitation. (A) Major river long profiles (from SRTM 90 m DEM; Lehner et al., 2008) with mean concavity (θ) and ksn shown. Locations in Fig. 2. (B) Topography and channel steepness (ksn; n = 382 rivers). Note systematic decrease in ksn downstream across the northern Upper Beni basin compared to the south. Inset profiles are 50 km wide swaths of mean annual precipitation across the Upper Beni Basin and the southern basins from the data in Fig. 2 inset. Note the increased magnitude and focused peak rainfall in the Upper Beni relative to the south.

APPENDIX

LONGITUDINAL PROFILE ANALYSIS

Past studies show that the 3 arc-second SRTM dataset is sufficient to characterize the channel profiles of large rivers (e.g., Kirby et al., 2003; Miller et al., 2012; Wobus et al., 2006a). To focus on long length-scale changes and to minimize DEM noise, I applied a 45-pixel streamwise moving average filter to the raw DEM data (after Kirby et al., 2003). For the individual river analysis, I sampled at 10 m vertical intervals for channel slope and contributing drainage area (after Snyder et al., 2000). For comparison between streams and to eliminate the autocorrelation between k_s and θ, I estimated a normalized steepness index (k_{sn}) by fitting the data with a fixed reference concavity (θ_{ref}) (e.g., Wobus et al., 2006a). Theoretically, θ_{ref} is assigned the regional mean θ for all equilibrium bedrock channels (Wobus et al., 2006a). However, studies show results are insensitive to the choice of θ_{ref} (Schoenbohm et al., 2004). For comparison with previous studies, I used $\theta_{ref} = 0.45$ (e.g., Cyr et al., 2010; Karlstrom et al., 2012; Ouimet et al., 2009; Safran et al., 2005; Schoenbohm et al., 2004; Snyder et al., 2000). To analyze regional steepness patterns, I calculated mean k_{sn} in a 0.5 km moving window along 252 rivers in southern Bolivia (Fig. 8A) and 130 rivers in the Upper Beni River Basin (Fig. 11B) (e.g., Cyr et al., 2010; Kirby and Whipple, 2001; Kirby et al., 2003; Snyder et al., 2000; Wobus et al., 2006a). Knickpoints at tributary junctions are disregarded because large increases in contributing drainage area can alter k_{sn} calculations.

REFERENCES

Allmendinger, R.W., Jordan, T.E., Kay, S.M., and Isacks, B.L., 1997, The evolution of the Altiplano-Puna Plateau of the Central Andes: Annual Review of Earth and Planetary Sciences, v. 25, p. 139-174, doi:10.1146/annurev.earth.25.1.139.

Armijo, A.V., Quiroga, F.H.G., Ontiveros, A.A., and Guarachi, J.C., compilers, 1996, Mapa Geológico de Bolivia: SERGEOMIN and YPFB, scale 1:1,000,000, 1 sheet.

Barke, R., 2004, Late Cenozoic tectonic and topographic evolution of the Bolivian Andes [Ph.D. thesis]: University of Oxford, 420 p.

Barke, R., and Lamb, S., 2006, Late Cenozoic uplift of the Eastern Cordillera, Bolivian Andes: Earth and Planetary Science Letters, v. 249, p. 350-367, doi:10.1016/j.epsl.2006.07.012.

Barnes, J.B., and Ehlers, T.A., 2009, End member models for Andean Plateau uplift: Earth-Science Reviews, v. 97, p. 105-132, doi:10.1016/j.earscirev.2009.08.003.

Barnes, J.B., and Pelletier, J.D., 2006, Latitudinal Variation of Denudation in the Evolution of the Bolivian Andes: American Journal of Science, v. 306, p. 1-31, doi:10.2475/ajs.306.1.1.

Barnes, J.B., Ehlers, T.A., McQuarrie, N., O'Sullivan, P.B., and Tawackoli, S., 2008, Thermochronometer record of central Andean Plateau growth, Bolivia (19.5°S): Tectonics, v. 27, p. TC3003, doi:10.1029/2007tc002174.

Barnes, J.B., Ehlers, T.A., Insel, N., McQuarrie, N., and Poulsen, C.J., 2012, Linking orography, climate, and exhumation across the central Andes: Geology, (in press).

Bookhagen, B., and Burbank, D.W., 2006, Topography, relief, and TRMM-derived rainfall variations along the Himalaya: Geophysical Research Letters, v. 33, p. L08405, doi:10.1029/2006gl026037.

Bookhagen, B., and Strecker, M.R., 2008, Orographic barriers, high-resolution TRMM rainfall, and relief variations along the eastern Andes: Geophysical Research Letters, v. 35, p. L06403, doi:10.1029/2007gl032011.

Bookhagen, B., and Strecker, M.R., 2012, Spatiotemporal trends in erosion rates across a pronounced rainfall gradient: Examples from the southern Central Andes: Earth and Planetary Science Letters, v. 327–328, p. 97-110, doi:10.1016/j.epsl.2012.02.005.

Brooks, B.A., Allmendinger, R.W., and de la Barra, I.G., 1996, Fault spacing in the El Teniente Mine, central Chile: Evidence for nonfractal fault geometry: Journal of

Geophysical Research-Solid Earth, v. 101, p. 13633-13653, doi:10.1029/96jb00800.

Burbank, D.W., and Anderson, R.S., 2011, Tectonic Geomorphology, John Wiley & Sons.

Clarke, B.A., and Burbank, D.W., 2011, Quantifying bedrock-fracture patterns within the shallow subsurface: Implications for rock mass strength, bedrock landslides, and erodibility: Journal of Geophysical Research-Earth Surface, v. 116, p. F04009, doi:10.1029/2011jf001987.

Cyr, A.J., Granger, D.E., Olivetti, V., and Molin, P., 2010, Quantifying rock uplift rates using channel steepness and cosmogenic nuclide-determined erosion rates: Examples from northern and southern Italy: Lithosphere, v. 2, p. 188-198, doi:10.1130/l96.1.

DiBiase, R.A., and Whipple, K.X., 2011, The influence of erosion thresholds and runoff variability on the relationships among topography, climate, and erosion rate: Journal of Geophysical Research-Earth Surface, v. 116, p. F04036, doi:10.1029/2011jf002095.

Dühnforth, M., Anderson, R.S., Ward, D., and Stock, G.M., 2010, Bedrock fracture control of glacial erosion processes and rates: Geology, v. 38, p. 423-426, doi:10.1130/g30576.1.

Dunn, J.F., Hartshorn, K.G., and Hartshorn, P.W., 1995, Structural styles and hydrocarbon potential of the sub-Andean thrust belt of southern Bolivia: AAPG Memoir, v. 62, p. 523-543.

Duvall, A., Kirby, E., and Burbank, D.W., 2004, Tectonic and lithologic controls on bedrock channel profiles and processes in coastal California: Journal of Geophysical Research-Earth Surface, v. 109, p. F03002, doi:10.1029/2003jf000086.

Ege, H., Sobel, E.R., Scheuber, E., and Jacobshagen, V., 2007, Exhumation history of the southern Altiplano plateau (southern Bolivia) constrained by apatite fission track thermochronology: Tectonics, v. 26, p. TC1004, doi:10.1029/2005tc001869.

Elger, K., Oncken, O., and Glodny, J., 2005, Plateau-style accumulation of deformation: Southern Altiplano: Tectonics, v. 24, p. TC4020, doi:10.1029/2004tc001675.

Flint, J.J., 1974, Stream gradient as a function of order, magnitude, and discharge: Water Resources Research, v. 10, p. 969-973.

Foster, M.A., and Kelsey, H.M., 2012, Knickpoint and knickzone formation and propagation, South Fork Eel River, northern California: Geosphere, v. 8, p. 403-416, doi:10.1130/ges00700.1.

Garreaud, R.D., and Wallace, J.M., 1997, The diurnal march of convective cloudiness over the Americas: Monthly Weather Review, v. 125, p. 3157.

Gillespie, P.A., Howard, C.B., Walsh, J.J., and Watterson, J., 1993, Measurement and characterization of spatial distributions of fractures: Tectonophysics, v. 226, p. 113-141, doi:10.1016/0040-1951(93)90114-y.

Goldrick, G., and Bishop, P., 2007, Regional analysis of bedrock stream long profiles: evaluation of Hack's SL form, and formulation and assessment of an alternative (the DS form): Earth Surface Processes and Landforms, v. 32, p. 649-671, doi:10.1002/esp.1413.

Goudie, A.S., 2006, The Schmidt Hammer in geomorphological research: Progress in Physical Geography, v. 30, p. 703-718, doi:10.1177/0309133306071954.

Gubbels, T.L., Isacks, B.L., and Farrar, E., 1993, High-level surfaces, plateau uplift, and foreland development, Bolivian central Andes: Geology, v. 21, p. 695-698, doi:10.1130/0091-7613(1993)021<0695:hlspua>2.3.co;2.

Hack, J.T., 1957, Studies of longitudinal stream profiles in Virginia and Maryland: U. S. Geological Survey Professional Paper, p. 45-97.

Haviv, I., Enzel, Y., Whipple, K.X., Zilberman, E., Matmon, A., Stone, J., and Fifield, K.L., 2010, Evolution of vertical knickpoints (waterfalls) with resistant caprock: Insights from numerical modeling: Journal of Geophysical Research-Earth Surface, v. 115, p. F03028, doi:10.1029/2008jf001187.

Horton, B.K., 1999, Erosional control on the geometry and kinematics of thrust belt development in the Central Andes: Tectonics, v. 18, p. 1292-1304.

Howard, A.D., and Kerby, G., 1983, Channel changes in badlands: Geological Society of America Bulletin, v. 94, p. 739-752.

Isacks, B.L., 1988, Uplift of the central Andean Plateau and bending of the Bolivian Orocline: Journal of Geophysical Research-Solid Earth and Planets, v. 93, p. 3211-3231.

Jansen, J.D., Codilean, A.T., Bishop, P., and Hoey, T.B., 2010, Scale Dependence of Lithological Control on Topography: Bedrock Channel Geometry and Catchment Morphometry in Western Scotland: The Journal of Geology, v. 118, p. 223-246, doi:10.1086/651273.

Johnson, J.P.L., Whipple, K.X., Sklar, L.S., and Hanks, T.C., 2009, Transport slopes, sediment cover, and bedrock channel incision in the Henry Mountains, Utah: Journal of Geophysical Research-Earth Surface, v. 114, p. F02014, doi:10.1029/2007jf000862.

Karlstrom, K.E., Coblentz, D., Dueker, K., Ouimet, W.B., Kirby, E., Van Wijk, J., Schmandt, B., Kelley, S., Lazear, G., Crossey, L.J., Crow, R., Aslan, A., Darling, A., Aster, R., MacCarthy, J., Hansen, S.M., Stachnik, J., Stockli, D.F., Garcia, R.V., Hoffman, M., McKeon, R., Feldman, J., Heizler, M., Donahue, M.S., and the CREST Working Group, 2012, Mantle-driven dynamic uplift of the Rocky Mountains and Colorado Plateau and its surface response: Toward a unified hypothesis: Lithosphere, v. 4, p. 3-22, doi:10.1130/l150.1.

Katz, O., Reches, Z., and Roegiers, J.C., 2000, Evaluation of mechanical rock properties using a Schmidt Hammer: International Journal of Rock Mechanics and Mining Sciences, v. 37, p. 723-728, doi:10.1016/s1365-1609(00)00004-6.

Kennan, L., Lamb, S.H., and Rundle, C., 1995, K-Ar dates from the Altiplano and Cordillera Oriental of Bolivia: implications for Cenozoic stratigraphy and tectonics: Journal of South American Earth Sciences, v. 8, p. 163-186, doi:10.1016/0895-9811(95)00003-x.

Kennan, L., Lamb, S.H., and Hoke, L., 1997, High-altitude palaeosurfaces in the Bolivian Andes: evidence for late Cenozoic surface uplift, *in* Widdowson, M., ed., Palaeosurfaces: Recognition, Reconstruction and Palaeoenvironmental Interpretation, Volume 120: Milton Keynes, United Kingdom, The Geological Society, London, p. 307-323.

Kirby, E., and Ouimet, W.B., 2011, Tectonic geomorphology along the eastern margin of Tibet: insights into the pattern and processes of active deformation adjacent to the Sichuan Basin, *in* Gloaguen, R., and Ratschbacher, L., eds., Growth and Collapse of the Tibetan Plateau, Geological Society, London, Special Publications 353, p. 165-188.

Kirby, E., and Whipple, K.X., 2001, Quantifying differential rock-uplift rates via stream profile analysis: Geology, v. 29, p. 415-418, doi:10.1130/0091-7613(2001)029<0415:qdrurv>2.0.co;2.

Kirby, E., and Whipple, K.X., in review, Expression of active tectonics in erosional landscapes: Journal of Structural Geology.

Kirby, E., Whipple, K.X., Tang Wenqing, and Chen Zhiliang, 2003, Distribution of active rock uplift along the eastern margin of the Tibetan Plateau: Inferences from bedrock channel longitudinal profiles: Journal of Geophysical Research-Solid Earth, v. 108, p. 2217, doi:10.1029/2001jb000861.

Kley, J., 1996, Transition from basement-involved to thin-skinned thrusting in the Cordillera Oriental of southern Bolivia: Tectonics, v. 15, p. 763-775, doi:10.1029/95tc03868.

Kley, J., 1999, Geologic and geometric constraints on a kinematic model of the Bolivian orocline: Journal of South American Earth Sciences, v. 12, p. 221-235, doi:10.1016/s0895-9811(99)00015-2.

Kley, J., Gangui, A.H., and Kruger, D., 1996, Basement-involved blind thrusting in the eastern Cordillera Oriental, southern Bolivia: Evidence from cross-sectional balancing, gravimetric and magnetotelluric data: Tectonophysics, v. 259, p. 171-184.

Lague, D., and Davy, P., 2003, Constraints on the long-term colluvial erosion law by analyzing slope-area relationships at various tectonic uplift rates in the Siwaliks Hills (Nepal): Journal of Geophysical Research-Solid Earth, v. 108, p. 2129, doi:10.1029/2002jb001893.

Lehner, B., Verdin, K.L., and Jarvin, A., 2008, New global hydrography derived from spaceborne elevation data: Eos (Transactions, American Geophysical Union), v. 89, p. 93-94.

Masek, J.G., Isacks, B.L., Gubbels, T.L., and Fielding, E.J., 1994, Erosion and tectonics at the margins of continental plateaus: Journal of Geophysical Research-Solid Earth, v. 99, p. 13941-13956, doi:10.1029/94jb00461.

McQuarrie, N., 2002, The kinematic history of the central Andean fold-thrust belt, Bolivia: Implications for building a high plateau: Geological Society of America Bulletin, v. 114, p. 950-963, doi:10.1130/0016-7606(2002)114<0950:tkhotc>2.0.co;2.

McQuarrie, N., and Davis, G.H., 2002, Crossing the several scales of strain-accomplishing mechanisms in the hinterland of the central Andean fold–thrust belt, Bolivia: Journal of Structural Geology, v. 24, p. 1587-1602, doi:10.1016/s0191-8141(01)00158-4.

McQuarrie, N., and DeCelles, P., 2001, Geometry and structural evolution of the central Andean backthrust belt, Bolivia: Tectonics, v. 20, p. 669-692, doi:10.1029/2000tc001232.

McQuarrie, N., Horton, B.K., Zandt, G., Beck, S., and DeCelles, P.G., 2005, Lithospheric evolution of the Andean fold–thrust belt, Bolivia, and the origin of the central Andean plateau: Tectonophysics, v. 399, p. 15-37, doi:10.1016/j.tecto.2004.12.013.

McQuarrie, N., Barnes, J.B., and Ehlers, T.A., 2008a, Geometric, kinematic, and erosional history of the central Andean Plateau, Bolivia (15–17°S): Tectonics, v. 27, p. TC3007, doi:10.1029/2006tc002054.

McQuarrie, N., Ehlers, T.A., Barnes, J.B., and Meade, B., 2008b, Temporal variation in climate and tectonic coupling in the central Andes: Geology, v. 36, p. 999-1002, doi:10.1130/g25124a.1.

Montgomery, D.R., Balco, G., and Willett, S.D., 2001, Climate, tectonics, and the morphology of the Andes: Geology, v. 29, p. 579-582, doi:10.1130/0091-7613(2001)029<0579:ctatmo>2.0.co;2.

Müller, J.P., Kley, J., and Jacobshagen, V., 2002, Structure and Cenozoic kinematics of the Eastern Cordillera, southern Bolivia (21°S): Tectonics, v. 21, p. 1037, doi:10.1029/2001tc001340.

Niemann, J.D., Gasparini, N.M., Tucker, G.E., and Bras, R.L., 2001, A quantitative evaluation of Playfair's law and its use in testing long-term stream erosion models: Earth Surface Processes and Landforms, v. 26, p. 1317-1332, doi:10.1002/esp.272.

Norton, K., and Schlunegger, F., 2011, Migrating deformation in the Central Andes from enhanced orographic rainfall: Nature Communications, v. 2, p. 584, doi:10.1038/ncomms1590.

Ouimet, W.B., Whipple, K.X., and Granger, D.E., 2009, Beyond threshold hillslopes: Channel adjustment to base-level fall in tectonically active mountain ranges: Geology, v. 37, p. 579-582, doi:10.1130/g30013a.1.

Roe, G.H., Montgomery, D.R., and Hallet, B., 2002, Effects of orographic precipitation variations on the concavity of steady-state river profiles: Geology, v. 30, p. 143-146, doi:10.1130/0091-7613(2002)030<0143:eoopvo>2.0.co;2.

Safran, E.B., Bierman, P.R., Aalto, R., Dunne, T., Whipple, K.X., and Caffee, M., 2005, Erosion rates driven by channel network incision in the Bolivian Andes: Earth Surface Processes and Landforms, v. 30, p. 1007-1024, doi:10.1002/esp.1259.

Schlunegger, F., Norton, K.P., and Zeilinger, G., 2011, Climatic Forcing on Channel Profiles in the Eastern Cordillera of the Coroico Region, Bolivia: Journal of Geology, v. 119, p. 97-107, doi:10.1086/657407.

Schmitz, M., and Kley, J., 1997, The geometry of the central Andean backarc crust: Joint interpretation of cross-section balancing and seismic refraction data: Journal of South American Earth Sciences, v. 10, p. 99-110, doi:10.1016/s0895-9811(97)00009-6.

Schoenbohm, L.M., Whipple, K.X., Burchfiel, B.C., and Chen, L., 2004, Geomorphic constraints on surface uplift, exhumation, and plateau growth in the Red River region, Yunnan Province, China: Geological Society of America Bulletin, v. 116, p. 895-909, doi:10.1130/b25364.1.

Seidl, M.A., and Dietrich, W.E., 1992, The problem of channel erosion into bedrock, *in* Schmidt, K.H., and de Ploey, J., eds., Functional Geomorphology: Landform Analysis and Models: Cremlingen-Destedt, Germany, Catena Supplement 23, p. 101-124.

Selby, M.J., 1980, A rock mass strength classification for geomorphic purposes: With tests from Antarctica and New Zealand: Zeitschrift für Geomorphologie, v. 24, p. 31-51.

Sklar, L.S., and Dietrich, W.E., 1998, River longitudinal profiles and bedrock incision models: Stream power and the influence of sediment supply, *in* Tinkler, J., and Wohl, E., eds., Rivers Over Rock: Fluvial Processes in Bedrock Channels, Volume 107: Washington, DC, AGU, p. 237-260.

Sklar, L.S., and Dietrich, W.E., 2001, Sediment and rock strength controls on river incision into bedrock: Geology, v. 29, p. 1087-1090, doi:10.1130/0091-7613(2001)029<1087:sarsco>2.0.co;2.

Snyder, N.P., Whipple, K.X., Tucker, G.E., and Merritts, D.J., 2000, Landscape response to tectonic forcing: Digital elevation model analysis of stream profiles in the Mendocino triple junction region, northern California: Geological Society of America Bulletin, v. 112, p. 1250-1263, doi:10.1130/0016-7606(2000)112<1250:lrttfd>2.0.co;2.

Snyder, N.P., Whipple, K.X., Tucker, G.E., and Merritts, D.J., 2003, Channel response to tectonic forcing: field analysis of stream morphology and hydrology in the Mendocino triple junction region, northern California: Geomorphology, v. 53, p. 97-127, doi:10.1016/s0169-555x(02)00349-5.

Stimpson, B., 1980, Intact rock strength and fracture spacing relationships in a porphyry copper deposit: International Journal of Rock Mechanics and Mining Sciences & Geomechanics Abstracts, v. 17, p. 67-68, doi:10.1016/0148-9062(80)90008-x.

Stock, J.D., and Montgomery, D.R., 1999, Geologic constraints on bedrock river incision using the stream power law: Journal of Geophysical Research-Solid Earth, v. 104, p. 4983-4993, doi:10.1029/98jb02139.

Stolar, D.B., Willett, S.D., and Roe, G.H., 2006, Climatic and tectonic forcing of a critical orogen: Geological Society of America Special Papers, v. 398, p. 241-250, doi:10.1130/2006.2398(14).

Tinkler, K.J., and Wohl, E.E., 1998, Rivers Over Rock: Fluvial Processes in Bedrock Channels: Washington, DC, AGU, Geophysical Monograph Series, 323 p.

van der Beek, P., and Bishop, P., 2003, Cenozoic river profile development in the Upper Lachlan catchment (SE Australia) as a test of quantitative fluvial incision models: Journal of Geophysical Research-Solid Earth, v. 108, p. 2309, doi:10.1029/2002jb002125.

VanLaningham, S., Meigs, A., and Goldfinger, C., 2006, The effects of rock uplift and rock resistance on river morphology in a subduction zone forearc, Oregon, USA: Earth Surface Processes and Landforms, v. 31, p. 1257-1279, doi:10.1002/esp.1326.

Walsh, L.S., Martin, A.J., Ojha, T.P., and Fedenczuk, T., 2012, Correlations of fluvial knickzones with landslide dams, lithologic contacts, and faults in the southwestern Annapurna Range, central Nepalese Himalaya: Journal of

Geophysical Research-Earth Surface, v. 117, p. F01012, doi:10.1029/2011jf001984.

Whipple, K.X., 2004, Bedrock Rivers and the Geomorphology of Active Orogens: Annual Review of Earth and Planetary Sciences, v. 32, p. 151-185, doi:10.1146/annurev.earth.32.101802.120356.

Whipple, K.X., 2009, The influence of climate on the tectonic evolution of mountain belts: Nature Geoscience, v. 2, p. 97-104, doi:10.1038/ngeo413.

Whipple, K.X., and Tucker, G.E., 1999, Dynamics of the stream-power river incision model: Implications for height limits of mountain ranges, landscape response timescales, and research needs: Journal of Geophysical Research-Solid Earth, v. 104, p. 17661-17674, doi:10.1029/1999jb900120.

Whipple, K.X., Kirby, E., and Brocklehurst, S.H., 1999, Geomorphic limits to climate-induced increases in topographic relief: Nature, v. 401, p. 39-43, doi:10.1038/43375.

Whipple, K.X., Hancock, G.S., and Anderson, R.S., 2000a, River incision into bedrock: Mechanics and relative efficacy of plucking, abrasion, and cavitation: Geological Society of America Bulletin, v. 112, p. 490-503, doi:10.1130/0016-7606(2000)112<490:riibma>2.0.co;2.

Whipple, K.X., Snyder, N.P., and Dollenmayer, K., 2000b, Rates and processes of bedrock incision by the Upper Ukak River since the 1912 Novarupta ash flow in the Valley of Ten Thousand Smokes, Alaska: Geology, v. 28, p. 835-838, doi:10.1130/0091-7613(2000)28<835:rapobi>2.0.co;2.

Whipple, K.X., DiBiase, R.A., and Crosby, B., in review, Bedrock Rivers, Treatise in Fluvial Geomorphology, Volume 9.29.

Whittaker, A.C., 2012, How do landscapes record tectonics and climate?: Lithosphere, v. 4, p. 160-164, doi:10.1130/rf.l003.1.

Whittaker, A.C., Attal, M., Cowie, P., Tucker, G., and Roberts, G., 2008, Decoding temporal and spatial patterns of fault uplift using transient river long profiles: Geomorphology, v. 100, p. 506-526, doi:10.1016/j.geomorph.2008.01.018.

Willett, S.D., 1999, Orogeny and orography: The effects of erosion on the structure of mountain belts: Journal of Geophysical Research-Solid Earth, v. 104, p. 28957-28981, doi:10.1029/1999jb900248.

Wobus, C.W., Whipple, K.X., Kirby, E., Snyder, N.P., Johnson, J., Spyropolou, K., Crosby, B., and Sheehan, D., 2006a, Tectonics from topography: Procedures, promise, and pitfalls, *in* Willett, S.D., Hovius, N., Brandon, M.T., and Fisher, D.M., eds., Tectonics, Climate, and Landscape Evolution: Boulder, Colorado, Geological Society of America Special Paper 398, p. 55-74.

Wobus, C.W., Tucker, G.E., and Anderson, R.S., 2006b, Self-formed bedrock channels: Geophysical Research Letters, v. 33, p. L18408, doi:10.1029/2006gl027182.

Wobus, C.W., Whipple, K.X., and Hodges, K.V., 2006c, Neotectonics of the central Nepalese Himalaya: Constraints from geomorphology, detrital 40Ar/39Ar thermochronology, and thermal modeling: Tectonics, v. 25, p. TC4011, doi:10.1029/2005tc001935.

Wobus, C.W., Tucker, G.E., and Anderson, R.S., 2010, Does climate change create distinctive patterns of landscape incision?: Journal of Geophysical Research-Earth Surface, v. 115, p. F04008, doi:10.1029/2009jf001562.

Zaprowski, B.J., Pazzaglia, F.J., and Evenson, E.B., 2005, Climatic influences on profile concavity and river incision: Journal of Geophysical Research-Earth Surface, v. 110, p. F03004, doi:10.1029/2004jf000138.